ELSEVIER

Journal of Molecular Catalysis A: Chemical 186 (2002) 79–88

JOURNAL OF MOLECULAR CATALYSIS A: CHEMICAL

www.elsevier.com/locate/molcata

Methanol decomposition over copper particles incorporated in the interlayer regions of zinc aluminum silicate hydroxide

Keiji Hashimot*, Naoji Toukai

Osaka Municipal Technical Institute, Morinomiya Joto-ku, Osaka 536-8553, Japan

Received 3 July 2001; received in revised form 24 August 2001; accepted 5 October 2001

Abstract

The decomposition of methanol over copper particles incorporated in the interlayer regions of zinc aluminum silicate hydroxide, reduced CuO/Zn–mica and Cu^{2+}/Zn–mica, was studied. CuO/Zn–mica reduced with H_2 is high active for the decomposition, compared with reduced Cu^{2+}/Zn–mica. Methanol is selectively converted at 200 °C to H_2 and CO in reduced CuO/Zn–mica, whereas the methanol decomposition over reduced Cu^{2+}/Zn–mica forms formaldehyde as a by-product. IR data support that the decomposition over reduced CuO/Zn–mica proceeds via copper methoxide and/or copper formate as an intermediate. An adsorption of NH_3 shows that the amount of the adsorption on reduced CuO/Zn–mica is about six times as large as that on reduced Cu^{2+}/Zn–mica. The results indicate the difficulty of the reduction of copper ion in Cu^{2+}/Zn–mica, compared with CuO/Zn–mica. These results support that the active site for methanol decomposition on reduced CuO/Zn–mica is metallic Cu in the interlayer regions of Zn–mica.

Keywords: Methanol decomposition; Mica; Copper oxide; Fine particles

1. Introduction

The decomposition of methanol, which is an endothermic reaction, is efficient as a chemical heat-pump [1–3], and its decomposition has attracted a great deal of considerable attention as a hydrogen supplier for fuel cell. In addition, the decomposition will proves to be a great use as a test reaction to study the catalytic properties and the studies on the decomposition are helpful to improve the catalysts for methanol synthesis. Therefore, there are many studies on the decomposition [4–13]. The conventional method in industrial methanol plants uses copper–zinc-based oxide catalyst under extreme reaction conditions, 250–300 °C, 5–10 MPa and low one-pass conversion of 15–20%. To improve the low one-pass conversion due to the limitation of thermodynamics, a lower temperature of the reaction is required; the lower temperature is able to attain a low cost of methanol synthesis. In addition, the activity and products of the methanol conversion over copper–zinc-based oxide catalyst are significantly changed by its preparation method, because the activity and chemisorption properties indicate a structure sensitivity [14–17]. Therefore, many preparation methods have been advocated to improve the catalytic activity [18–21]. However, these improvements are not always adequate to attain a reaction temperature less than 200 °C. Furthermore, the most suitable structure and reaction field for methanol synthesis and its reverse reaction are still obscure in a copper–zinc oxide catalyst. On the other hand, we have reported that the fine particles of metal oxides incorporated into the

* Corresponding author. Tel.: +81-6963-8031; fax: +81-6963-8040.

1381-1169/02/$ – see front matter
PII: S1381-1169(01)00416-2

nanospace such as zeolite cavities and interlayer regions of clays, improve their catalytic properties like activity and selectivity [22–26]. Zinc aluminosilicate hydroxide of the formula $[Zn_3(Si_3Al)O_{10}(OH)_2]^-$ has a layer structure similar to that of mica; magnesium ions of phlogopite are substituted for zinc ions in zinc aluminosilicate hydroxide. The interlayer regions should be effective for the incorporation of fine particles of metal oxides, as expected. In addition, we have already revealed that potassium form zinc aluminosilicate hydroxide is very effective for a selective dehydrogenation of alcohols [27]. We have hence attempted the application of the layer compound of zinc oxide, zinc aluminosilicate hydroxide, to the catalyst for the decomposition of methanol. We have prepared the particles of copper oxide incorporated into the interlayer regions of zinc aluminum silicate hydroxide, CuO/Zn–mica, and studied on the decomposition of methanol. In this paper, we report: (1) decomposition of methanol over reduced CuO/Zn–mica and Cu^{2+}/Zn–mica; (2) high activity of reduced CuO/Zn–mica; (3) characterization of reduced CuO/Zn–mica and Cu^{2+}/Zn–mica.

2. Experimental

2.1. Materials

All chemicals used were commercial materials of analytical grade and used without further purification. Colloidal silica containing 18 wt.% of SiO_2 and less than 0.5 wt.% of sodium (Nissan Chemical Industry) was used without further purification; its commercial name is Snowtex N.

2.2. Preparation of potassium zinc aluminum silicate hydroxide, Zn–mica

Potassium hydroxide, 310 g (5.5 moles), was dissolved in 500 ml of deionized water. Aluminum nitrate hydrate, 65.0 g (0.175 moles), and zinc nitrate hydrate, 180.0 g (0.605 moles), were dissolved in 400 ml of deionized water. The solution of aluminum and zinc nitrate was then added to the potassium hydroxide solution, and a transparent mixture of aluminum and zinc hydroxides which is soluble in potassium hydroxide solution was obtained. The transparent solution was added to the colloidal silica, 220 g, containing 0.66 moles of SiO_2 and the resulting sol was allowed to age over night. The sol was taken place in 2-l of an autoclave and crystallized at 150 °C for a week. The resulting slurry of mica crystalline was filtered, washed several times with deionized water, and dried at 150 °C for 3 h.

2.3. Preparation of the catalyst, CuO/Zn–mica

Two grams of copper nitrate hydrate was dissolved into 100 ml of deionized water. Zn–mica, 2 g, was suspended in the solution, and potassium ion in Zn–mica was ion-exchanged at 50 °C for 3 h with Cu^{2+}. The resulting slurry of the Zn–mica was filtered and washed with deionized water. The ion-exchanged Zn–mica, Cu^{2+}/Zn–mica, were then dried at 150 °C for 5 h. The ion-exchanging and drying changed the color from white to blue; the resulting blue powder is Cu^{2+}/Zn–mica. Moreover, Cu^{2+}/Zn–mica was exposed at room temperature for 48 h to moist ammonia gas, and then calcinated at 400 °C for 5 h. The treatments changed the color from blue to dark gray; now the calcinated dark gray powder is described as CuO/Zn–mica. The BET surface area of the catalyst, CuO/Zn–mica, is 41 m^2/g. The chemical components are analyzed using a inductively coupled plasma (ICP) method and summarized in Table 1.

2.4. Preparation of copper oxides

The powder of copper hydroxide was treated in vacuo at 400 °C for 2 h prior to methanol conversion, till the powder gave no decomposition gas. The sample was then used to converse methanol.

Table 1
Chemical composition of the catalyst

Catalyst	Composition (wt.%)				
	K	Cu	Al	Zn	Si
CuO/Zn–mica	1.3	4.6	4.9	36	15
	0.0[a]	5.9[a]	5.0[a]	35.9[a]	15.6[a]
Cu^{2+}/Zn–mica	1.5	4.7	4.9	36	16

[a] Value calculated from the formula: $(CuO)_{1/2}[Zn_3(Si_3Al)O_{10}(OH)_2]$.

2.5. Decomposition of methanol to hydrogen and carbon monoxide

Decomposition was carried out at 200 °C in a constant volume of a quartz reaction tube, which was connected to a vacuum line. A catalyst of 0.020 g was weighted in the reactor. The catalyst was evacuated for 2 h at 250 °C. The catalyst was reduced at 250 °C for 1 h with H_2 prior to the decomposition of methanol. The catalyst was cooled to a fixed temperature after degassing H_2 and exposed at the same temperature to a fixed pressure of methanol vapor. The decomposition rate was measured by an increase in reaction pressure. The analyses of the decomposition products were performed using GC connected with a pulse micro-catalytic reactor with a helium-flow rate or a hydrogen-flow one of 10 ml min^{-1}. The amount of produced hydrogen was determined on the basis of the yield of CO, formaldehyde and methyl formate, because the intensity of the GC peak due to H_2 was not always accurate in the He carrier. Quartz tube has no contribution to the decomposition under the conditions.

2.6. X-ray photoelectron spectroscopy (XPS) measurements

XPS spectra of CuO/Zn–mica were obtained using a Shimadzu XPS-850 photoelectron spectrometer equipped with an Mg Kα X-ray source ($h\nu = 1253.6$ eV). The X-ray power supply was operated at 8 kV and 30 mA. During the measurements, the pressure inside the sample chamber was high (0.5×10^{-6} Pa). About 0.2 g of the catalyst was compressed at 2 t cm^{-2} using a pellet die to form circular disks that were ca. 1 mm thick and had a 5 mm diameter. All samples were dried for 5 h at 150 °C and fixed to the sample holder using double-sided adhesive tape. The graphite carbon XPS peak (C 1s) added to the sample was used as the calibration. For exact charge correction, calibration peak (C 1s) was measured before and after every XPS measurement.

2.7. X-ray powder diffraction (XRD)

XRD patterns of the samples were recorded using a McScience XP_{18} spectrometer (Ni-filtered Cu Kα, 40 kV, 50 mA). The sample was mounted on sample board and the measurements were immediately performed. XRD peak positions were corrected using the peak resulting from Si powder as calibrator.

2.8. FT-IR measurement

FT-IR spectra were recorded on a Shimadzu FT-IR 8100 using a conventional IR cell connected to a vacuum line and adsorption apparatus. The sample (0.01 g) was pressed at 7.5 t cm^{-2} using a pellet die to form a wafer with a 10 mm diameter and placed into the in situ IR cell allowing heat under a vacuum. After the wafer was heated in vacuo for 1 h, the wafer was treated at 250 °C for 1 h with H_2, and hydrogen was then degassed. The sample was cooled to 200 °C and exposed to methanol vapor (0.2 kPa) at 200 °C. FT-IR spectra of the sample adsorbed methanol were then recorded at room temperature.

2.9. CO_2-temperature-programmed desorption (CO_2-TPD)

CO_2-TPD measurements were recorded using a RUBOTHERM PRÄZISIONSMESSTECHNIK GMBH. The catalyst, about 70 mg, was exactly weighted and evacuated at 250 °C for 2 h. The catalyst was reduced at 250 °C for 1 h with H_2. Hydrogen was degassed at 250 °C till the weight of the catalyst became a constant which was used as a zero-adsorption weight. The catalyst was cooled and then exposed to CO_2 at 50 °C under the pressure of 1.8 kPa of CO_2. After the adsorption equilibrium was attained, carbon dioxide was evacuated at 50 °C till the sample weight became a constant. The sample was then heated in vacuo at 3 °C min^{-1} up to 200 °C. An amount of irreversible adsorption of carbon dioxide was determined on the basis of the overweight from the zero-adsorption weight.

2.10. NH_3-temperature-programmed desorption (NH_3-TPD)

NH_3-TPD was carried out using the same apparatus as that in CO_2-TPD. Cu/Zn–mica, about 70 mg, was exactly weighted and pretreated by the same procedure as that in CO_2-TPD. The sample was then exposed to NH_3 at 100 °C and 1.2 kPa of NH_3 pressure. After the adsorption equilibrium was attained, the

sample was evacuated at 100 °C till the weight of the adsorbed sample became a constant. The sample was then heated in vacuo at 3 °C min^{-1} up to 350 °C. The amount of the irreversible adsorption of NH_3 was also determined on the basis of the overweight from a zero-adsorption weight.

2.11. ESR measurement

ESR spectra of the catalysts were recorded at room temperature and at −150 °C by a JES-RE2X ESR spectrometer. The sample (0.20 g) was placed in a conventional cell-equipped ESR cavity. The cell was connected to a vacuum line, and the sample was treated in vacuo for 3 h at 350 °C prior to the ESR measurement. Manganese ions were used to measure the g-anisotropy of the ESR-active species as a standard marker.

3. Results and discussions

The decomposition and conversion of methanol over CuO/Zn–mica, CuO/Zn–mica(R), Cu^{2+}/Zn–mica and Cu^{2+}/Zn–mica(R) were studied; CuO/Zn–mica(R) and Cu^{2+}/Zn–mica(R) represent that CuO/Zn–mica and Cu^{2+}/Zn–mica have been reduced at 250 °C for 1 h with H_2, respectively. These results were summarized in Table 2. The decomposition over CuO/Zn–mica(R) selectively forms H_2 and CO, whereas that over Cu^{2+}/Zn–mica(R) gives formaldehyde as a by-product. Moreover, the conversion of methanol over copper oxide gives H_2, CO, methyl formate and formaldehyde. These main products agree with those on copper oxide reported in Refs. [28–32]. The product distribution in CuO/Zn–mica(R) is clearly different from that in CuO/Zn–mica, while the distinctive distribution on Cu^{2+}/Zn–mica remains to some extent in Cu^{2+}/Zn–mica(R), though the reduction of the catalysts significantly decreases the formation of methyl formate (Table 2). The difference of the product distribution strongly suggests the different reduction states of copper in both CuO/Zn–mica(R) and Cu^{2+}/Zn–mica(R). The decomposition of methanol and the formation of methyl formate occur in Zn–mica under the same conditions, though their rates are slow. These results lead to the conclusion that the load of copper on Zn–mica significantly enhances the decomposition except for CuO/Zn–mica.

Table 2
Decomposition products of methanol[a]

Catalyst	Conversion (mol%)	Products (mol%)			
		H_2	CO	MF	FA
CuO/Zn–mica	11[b]	57.4[b]	9.3[b]	5.6[b]	27.7[b]
CuO/Zn–mica(R)	41	66.7	33.3	0	0
Zn–mica	10	66.7	23.1	10.2	0
CuO	30	65.5	15.7	15.1	3.7
Cu^{2+}/Zn–mica	28	63.0	12.4	13.8	10.8
Cu^{2+}/Zn–mica(R)	23	59.2	17.3	1.0	22.5

[a] Decomposition temperature: 200 °C; R: prereduced at 250 °C for 1 h with H_2; MF: methyl formate; FA: formaldehyde. Catalyst: 0.015 g; injection amount of methanol: 2.1×10^{-6} moles.
[b] Decomposition at 250 °C.

The decomposition rates over CuO/Zn–mica(R) were studied at 170, 180 and 200 °C under a constant pressure of 4.0 kPa of methanol and shown in Fig. 1. Moreover, the decomposition rate over CuO/Zn–mica(R) is about two times as faster as the total ones of the methanol decomposition and formaldehyde formation over Cu^{2+}/Zn–mica(R) under the same conditions (Table 2). The decomposition rate nearly corresponds to that of high active Pd/CeO_2 catalyst reported by Schen and Matsumura [33]. The high decomposition rate hence leads to the conclusion that copper particles formed by reduction of copper oxide on Zn–mica promote the decomposition.

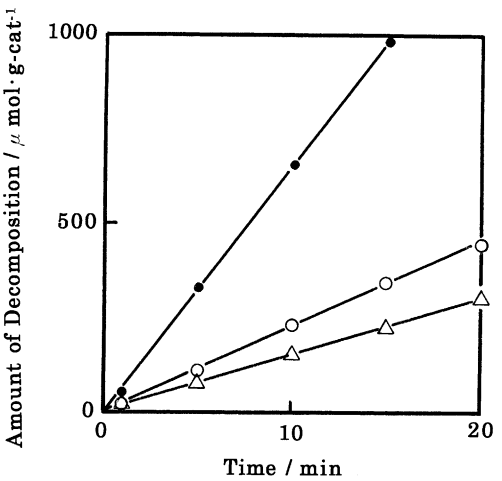

Fig. 1. Decomposition of methanol over reduced CuO/Zn–mica: 170 °C (△), 180 °C (○), 200 °C (●). Vapor pressure of methanol: 4.0 kPa.

The apparent activation energy for the decomposition over CuO/Zn–mica(R) was determined to be 96 kJ mol^{-1} on the basis of Arrhenius plots of the data in Fig. 1. The apparent activation energies for methanol synthesis on Cu(1 0 0) (68.6 ± 4.2 kJ mol^{-1}) [14], Cu(polycrystalline copper foil) (76.1 ± 10.5 kJ mol^{-1}) [16] and Cu(1 1 0) (∼67.8 kJ mol^{-1}) [15] were reported and the catalytic activity of the Cu particles in real Cu/ZnO catalysts might also be expected to resemble Cu(1 1 0) plane [15]. The obtained value for methanol decomposition is rather large, compared with those for methanol synthesis over metallic copper, but is reasonable, because methanol synthesis is exothermic. Furthermore, the obtained value is lower than that, 129.3 kJ mol^{-1} [34], for the decomposition of copper formate on Cu(1 1 0) plane; the decomposition of copper formate is often rate-limiting step in the copper–zinc oxide catalysts. The value suggests that the active site for methanol decomposition on CuO/Zn–mica(R) is metallic Cu, and the metallic Cu in the interlayer regions of Zn–mica accelerates the decomposition of copper formate.

Analyses of XPS of CuO/Zn–mica were carried out and the spectroscopy is shown in Fig. 2. The binding energy of copper loaded on the Zn–mica was determined and its XPS parameters are summarized in Table 3. The binding energies of Cu($2P_{3/2}$) in copper metal, Cu^{2+}, Cu_2O and CuO are 932.4, 934–937, 932.2 and 933.4 eV, respectively [35]. The value obtained is assigned to the binding energy of Cu($2P_{3/2}$) in copper oxide. In fact, the products and

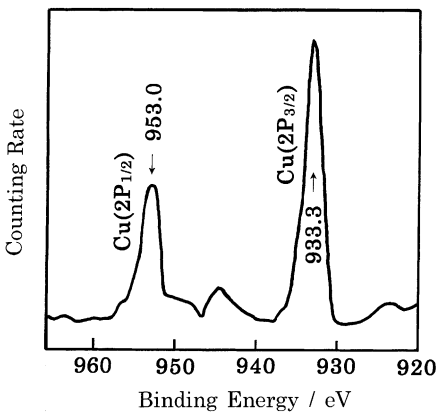

Fig. 2. Binding energy of Cu($2P_{3/2}$) and Cu($2P_{1/2}$) in CuO/Zn–mica.

Table 3
XPS parameters[a]

Catalyst	BE of Cu($2P_{3/2}$) (eV)	HW of Cu($2P_{3/2}$) (eV)	Cu content (mol%)
CuO/Zn–mica	933.3	2.2	1.4
CuO[b]	933.4	3.8	50

[a] BE: binding energy; HW: half width.
[b] Ref. [35].

their distribution on CuO/Zn–mica resemble those on copper oxide (Table 2). It is hence concluded that the treatment of Cu^{2+}/Zn–mica with NH_3 and its post-calcination transform Cu^{2+} ions to copper oxide.

X-ray powder diffraction patterns of CuO/Zn–mica were recorded and shown in Fig. 3. The patterns well agree with those for potassium zinc aluminum silicate hydroxide in literature [36]. The space distance, *d*(0 0 1), is determined to be 1.02 nm. The space distance is larger than that expected from a diameter, 0.174 nm, of Cu^{2+} ion. The expansion of the space distance supports the intercalation of the fine particles of copper oxide in the interlayer regions of Zn–mica. No patterns due to copper oxides are observed. The results support high dispersion of copper oxides in the interlayer regions. The crystal size of Zn–mica was determined to be 29 nm from the half width of the peaks at (1 0 0), and (3 0 0), and 37 nm from that at (1 3 1) and (1 3 2), using Scherrer's equation [37].

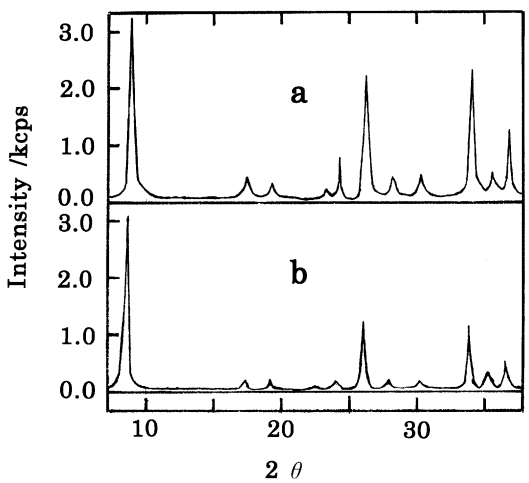

Fig. 3. X-ray powder diffraction patterns: (a) potassium form of Zn–mica; (b) CuO/Zn–mica.

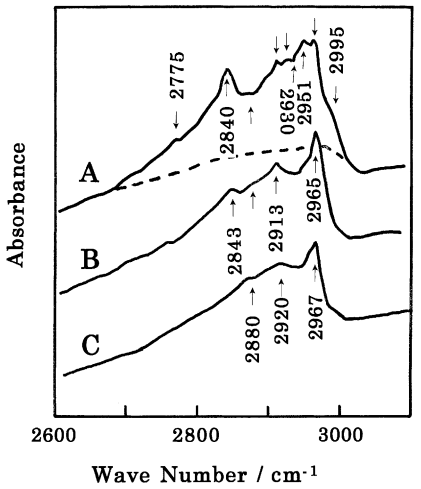

Fig. 4. FT-IR spectra of methanol adsorbed on reduced CuO/Zn–mica. Dotted line evacuation for 3 h at 350 °C; (A) exposure of CuO/Zn–mica(R) at 200 °C for 15 min to 0.20 kPa of methanol vapor; (B) degassing (A) at room temperature for 30 s; (C) degassing (B) at 200 °C for 1 h.

FT-IR spectra of methanol adsorbed on CuO/Zn–mica(R) were recorded and shown in Fig. 4. The adsorption of methanol at 200 °C on CuO/Zn–mica(R) gives the bands at 2965 cm^{-1} (with a shoulder at 2995 cm^{-1}), 2951 cm^{-1} (with a shoulder around 2940 and 2930 cm^{-1}), 2913 cm^{-1} (with a shoulder around 2880 cm^{-1}), 2840 cm^{-1} (with a shoulder around 2815 cm^{-1}), around 2775 and 2700 cm^{-1}. The methyl group gives rise to a moderately strong band in the 3000–2840 cm^{-1} region [38]. In literature [39–48], Infrared absorption, arising from C–H stretching vibration in CH_3O–Cu, copper formate and physisorbed methanol on copper, occurs in the general region around 2996–2787 cm^{-1}: CH_3O–Cu [1 1 0], 2940, 2840 cm^{-1} [40]; CH_3O–Cu[1 0 0], 2910, 2830 cm^{-1} [39]; 2901, 2861 and 2787 cm^{-1} [43]; CH_3O–Cu[polycrystalline copper], 2926, 2815 cm^{-1} [42]; CH_3O–Cu, 2930, 2821 cm^{-1} [42]; HCOO–Cu, 2930, 2850, 1620, 1350 cm^{-1} [44,45]; bidentate formate species on copper, 2926, 2842 cm^{-1} [46], 2937, 2857 cm^{-1} [46]and 2936 2853 cm^{-1} [42]; bridging formate species on copper, 2933, 2906 (shoulder), 2833 cm^{-1} [46]; and 2938, 2843 cm^{-1} [46]; physisorbed methanol on copper, 2996, 2960 and 2859 cm^{-1} [47]; 2995, 2959, 2854 cm^{-1} [42], and 2955 and 2845 cm^{-1} [48]. In addition, infrared absorption, arising from C–H stretching vibration in CH_3O–Zn and zinc formate, occurs in the general region around 2970–2740 cm^{-1}: CH_3O–Zn; 2930, 2825 cm^{-1} [45]; HCOO-Zn, 2970, 2880, 2740 cm^{-1} [45]. A 30 s degassing of the sample of methanol adsorption at room temperature significantly decreased the intensities of the bands at 2995, 2951 and 2840 cm^{-1} and remained the bands at 2965, 2913 cm^{-1} (with a shoulder around 2930 cm^{-1}), 2843 cm^{-1} (with a shoulder around 2830 and 2815 cm^{-1}), and 2775 cm^{-1}. The results indicate that the bands at 2995, 2951 and 2840 cm^{-1} are assigned at the stretching vibrations of C–H bond in physisorbed methanol on copper. The bands at 2930, 2843 and 2775 cm^{-1} are attributed to a stretching vibration of C–H in copper methoxide and/or bridging formate species on copper. A 1 h degassing of the sample at 200 °C resulted in a disappearance of the bands at 2930, 2843 and 2775 cm^{-1}, and remained the bands at 2967, around 2920, and 2880 cm^{-1} (with a shoulder around 2830 cm^{-1}), although their intensities decreased. The bands around 2920 and 2830 cm^{-1} are attributable to a stretching vibration of C–H in zinc methoxide. The bands at 2967 and 2880 cm^{-1} due to strong adsorption species are attributed to a stretching vibration of C–H in zinc formate. These results lead to the conclusion that the decomposition over CuO/Zn–mica(R) proceeds via copper methoxide and/or copper formate as an intermediate. It is well known that the methanol synthesis over the conventional catalysts containing copper and zinc oxide proceeds via formate species as an intermediate [49–55]. However, the opinions have been divided on the matter of the role of the individual components in copper-based methanol synthesis catalyst. Burch et al. [49–51] reported that the nature of the oxide support is critical in determining the overall methanol synthesis activity. They explained the observation result in terms of the ability of the support to supply dissociated hydrogen which should have a substantial effect on the activity as the rate-determining step for methanol synthesis was the hydrogenation of copper formate. Waugh and coworkers [52–55] reported the importance of special sites located at the interface between copper and zinc oxide; methanol synthesis proceeds via formate species on the special sites. The structure of zinc aluminum silicate hydroxide has

layers consisting of a monolayer of octahedral zinc oxide and two pieces of tetrahedral silica–alumina monolayers, that is, a monolayer of octahedral zinc oxide is sandwiched by two pieces of silica–alumina monolayers. The six-membered rings of O^2-occupied a corner of tetrahedral silica and/or alumina are regularly arranged in the layer surface and the center of six-membered ring is a hole. The monolayer of zinc oxide crops out in the bottom of the hole. It is reasonably considered that the particles of copper in CuO/Zn–mica(R) are located at the center of the hole; each particle of copper is overcanopied by the upper layer consisting of the six-membered ring and zinc oxide. Considering the intercalation of methoxy and/or formate species in the rigid small space between copper particle and canopy, copper methoxide and formate formed on the particles of copper must be interacted by zinc oxide in the canopy, because the distance between copper particle and zinc oxide in the canopy may be approximately 0.3–0.5 nm although the distance depends on the particle size of copper. Therefore, the configurations are a similar to those at the special sites in the interface of the catalyst containing copper and zinc oxide in Refs. [54,55]. The reasonable configuration in CuO/Zn–mica(R) suggests the importance of the special sites similar to those in the interface of the catalyst containing copper and zinc oxide.

NH_3-TPD was studied and the results were shown in Table 4. The results indicate the presence of week acid sites in Zn–mica. The load of copper on the Zn–mica significantly increases the amount of NH_3 adsorption. The amount of NH_3 adsorption on CuO/Zn–mica(R) is larger than that on Cu^{2+}/Zn–mica(R). The adsorption amount at 100 °C is 9.8 mg (g-cat)$^{-1}$ (0.61 mmol (g-cat)$^{-1}$) in CuO/Zn–mica(R), whereas that is 2.1 mg (g-cat)$^{-1}$ in Cu^{2+}/Zn–mica(R). The amounts of copper loaded are 0.72 and 0.74 mmol (g-cat)$^{-1}$ in CuO/Zn–mica(R) and Cu^{2+}/Zn–mica(R), respectively. Assuming that the increase in the amount of NH_3 adsorption is due to adsorption of NH_3 on copper, the number of NH_3 adsorption per a copper atom is calculated to be 0.81 and 0.14 NH_3 molecule in CuO/Zn–mica(R) and Cu^{2+}/Zn–mica(R), respectively. In CuO/Zn–mica(R), the number of NH_3 adsorption for a copper atom is nearly equal to one molecule and is about six times as much as that in Cu^{2+}/Zn–mica(R). It is well known that an isolated copper ion is reduced to metal under very severe conditions, compared with copper oxide and cluster of copper oxide [56]. On reducing Cu^{2+}/Zn–mica with H_2, protons, equivalent to the reduction amount of Cu^{2+} to Cu^0, form to neutralize a charge of Zn–mica, whereas protons have been already present in CuO/Zn–mica, because the protons form on post-calcination of Cu^{2+}/Zn–mica pretreated with moist ammonia. The formed protons should increase the amount of the NH_3 adsorption. The difference of the amount of NH_3 adsorption between CuO/Zn–mica(R) and Cu^{2+}/Zn–mica(R) can be hence explained in terms of the difference of the amount of copper metal in both the catalysts. The results support the difficulty of the reduction of copper ion in Cu^{2+}/Zn–mica. In fact, the distinctive products in Cu^{2+}/Zn–mica remain still in Cu^{2+}/Zn–mica(R), although the formation of methyl formate decreases remarkably (Table 2).

Dehydrogenation of alcohols is well known to be a base–catalyst reaction. CO_2-TPD was studied and the results are shown in Table 5. Zn–mica have both acidic and basic sites as acid–base bifunctional catalysts and the dehydrogenation due to the basic sites is thus preferred to the dehydration due to the acid sites [27]. Little change of the amount of CO_2 adsorption

Table 4
Amount of carbon dioxide irreversibly adsorbed on CuO/Zn–mica[a]

Adsorption temperature (°C)	Amount of adsorbed CO_2 (mg (g-cat)$^{-1}$)		
	Cu^{2+}/Zn–mica(R)	CuO/Zn–mica(R)	Zn–mica
50	0.70	2.1	0.93
100	0.22	1.5	0.08
150	0.00	1.3	0.00

[a] R: reduced at 250 °C for 1 h with H_2.

Table 5
Amount of irreversible adsorption of NH_3 on CuO/Zn–mica[a]

Adsorption temperature (°C)	Amount of NH_3 adsorption (mg (g-cat)$^{-1}$)		
	CuO/Zn–mica(R)	Cu^{2+}/Zn–mica(R)	Zn–mica
100	9.8	2.1	0.53
150	5.4	1.5	0.00
200	2.5	0.77	–

[a] R: reduced at 250 °C for 1 h with H_2.

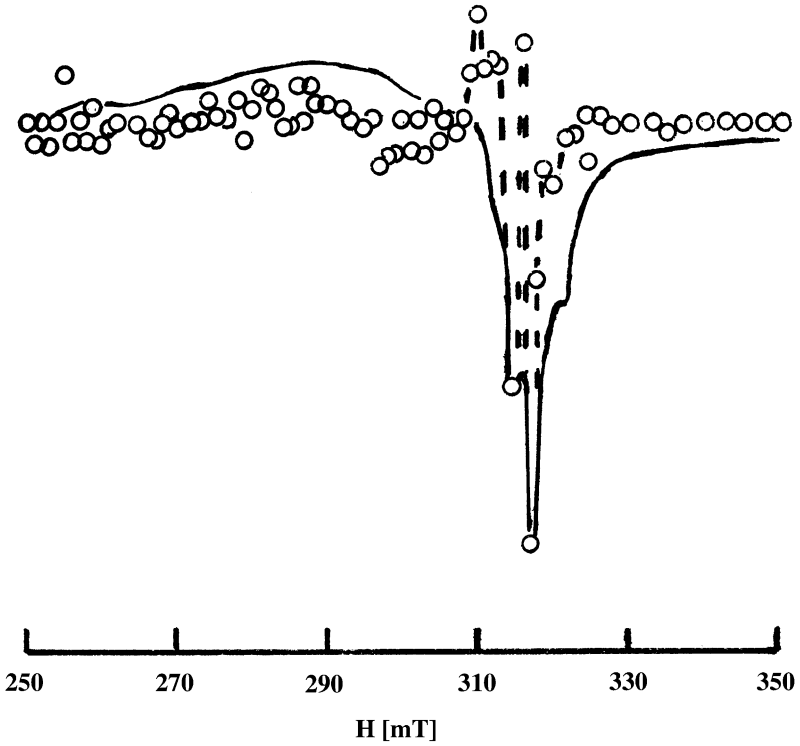

Fig. 5. Experimental and computed line shape of CuO/Zn–mica. Spectrum (dotted line) is superimposed by two lines computed with $A_{\parallel} = -0.0167$, $A_{\perp} = -0.0022$, $g_{\parallel} = 2.19$, $g_{\perp} = 2.055$ and with $A_{\parallel} = -0.0169$, $A_{\perp} = -0.0019$, $g_{\parallel} = 2.22$, $g_{\perp} = 2.057$; the ratio of the former to the latter is 4:3. Experimental spectrum (solid line) was recorded at $9.18\,\mathrm{Gc\,s^{-1}}$.

is observed in Cu^{2+}/Zn–mica(R), compared with Zn–mica, whereas the amount of CO_2 adsorption increases in CuO/Zn–mica(R). The increase in the amount of CO_2 adsorption supports the idea that a basic site of CuO/Zn–mica(R) increases, compared with Cu^{2+}/Zn–mica(R).

The ESR spectrum of CuO/Zn–mica were recorded and shown in Fig. 5. The ESR spectrum for CuO/Zn–mica shows two kinds of signals. One is a broad peak in the wide range 260–340 mT, and the perpendicular components are not well resolved. The other is an anisotropic strong peak to be $g_1 = 2.058$, $g_2 = 2.03$, $g_3 = 2.011$. Moreover, these signals are not observed in the absence of copper. ESR signals assigned to Cu^{2+} generally occur in the range of $g_1 = 2.4$, and $g_2 = g_3 = 2.1$ [57], whereas one assigned to O_2^- adsorbed on divalent metal ions are $g_1 = 2.05$ [58]. The observed line shape of the broad peak is typical for a polycrystalline sample containing Cu^{2+} in a site of axial symmetry. A first derivative curve was calculated according to the usual simulation method [59,60] at 10 G ($1G = 10^{-4}$ T) in a magnetic field of 250–350 mT. The intensity of the microwave absorption at each resonance field was obtained by numerical integration at interval of 1.5° to θ for all directions under an assumption of Lorentzian line shape function. The relevant components of the g and A tensors are presented in Table 6. An error of ± 0.0001 is appropriate for $A_{\perp}$ and $A_{\parallel}$, respectively. In literature [61,62], ESR spectra for an atomic state of Cu^{2+} ion such as Cu^{2+} in zeolite and copper oxide highly dispersed on alumina [63,64], gives a broad peak which has the components of $g_{\parallel} = 2.19$–2.40, $g_{\perp} = 2.055$–2.08, $0.018 > A_{\parallel} > -0.017$ and $0.0026 > A_{\perp} > -0.0022$. The observed line shape and its relevant components are very similar to those

Table 6
Spin Hamiltonian parameters for Cu^{2+} ion in CuO/Zn–mica

Sample	$g_\perp$	$g_\parallel$	$A_\perp$	$A_\parallel$
CuO/Zn–mica	2.055–2.057	2.19–2.22	−0.0022 to −0.0019	−0.0169 to −0.0167

for the state of highly dispersed copper. The results support the idea that copper oxide in CuO/Zn–mica is highly dispersed in the interlayer regions of Zn–mica as a fine particle. The peak of $g_1 = 2.058$, $g_2 = 2.03$, and $g_3 = 2.011$ is attributable to O_2^- attached to Cu^{2+} in the interlayer regions of Zn–mica.

4. Conclusion

The decomposition over CuO/Zn–mica(R) selectively forms H_2 and CO, whereas the decomposition over Cu^{2+}/Zn–mica(R) gives formaldehyde as a by-product. The load of copper on the Zn–mica enhances the decomposition. In particular, CuO/Zn–mica(R) is higher active for the decomposition, compared with Cu^{2+}/Zn–mica(R). The amount of CO_2 adsorption on Cu^{2+}/Zn–mica(R) is nearly equal to that on Zn–mica, whereas that on CuO/Zn–mica(R) increases. The increase in the amount of CO_2 adsorption supports an increase in a basic site of CuO/Zn–mica(R), compared with Cu^{2+}/Zn–mica(R). The amount of NH_3 adsorption on CuO/Zn–mica(R) is about six times as large as that in Cu^{2+}/Zn–mica(R). The difference between the amounts of NH_3 adsorption in CuO/Zn–mica(R) and Cu^{2+}/Zn–mica(R) can be explained by means of the difference between the amounts of copper metal in both the catalysts. The results support that the active site for methanol decomposition is metallic Cu in CuO/Zn–mica(R). The binding energy of $Cu(2P_{3/2})$ indicates that the loaded copper exists as copper oxide in CuO/Zn–mica. The XRD spectra for CuO/Zn–mica indicate an expansion of the interlayer distance of Zn–mica and so support a high dispersion of copper oxide in the interlayer regions. The spin Hamiltonian parameters for the ESR spectra of Cu^{2+} in CuO/Zn–mica also support a high dispersion of copper oxide in the interlayer regions of Zn–mica. The results lead to the conclusion that copper oxide exists in the interlayer regions of Zn–mica as fine particles. IR spectra for methanol adsorption on CuO/Zn–mica(R) indicate that the adsorption of methanol forms copper methoxide and/or copper formate. It is hence concluded that the decomposition over CuO/Zn–mica(R) proceeds via copper methoxide and/or copper formate as an intermediate. The reasonable configuration copper methoxide or copper formate in CuO/Zn–mica(R) suggests the importance of the special sites similar to those in the interface between copper and zinc oxide in the conventional catalyst containing copper and zinc oxide.

References

[1] H. Shirvani, C.E. Coering, S.C. Sorenson, SAE Paper No. 810681, 1981.
[2] E. Holmer, P.S. Berg, B.-I. Bertilsson, SAE Paper No. 800644, 1980.
[3] Catalysis Looks to the Future, National Research Council, National Academy Press, Washington, DC, 1992.
[4] M.S. Brogan, J.A. Cairns, T.J. Dines, C.H. Rochester, Spectrochim. Acta A 53 (7) (1997) 943.
[5] D.A. Chen, C.M. Friend, J. Phys. Chem. B 101 (29) (1997) 5712.
[6] Y. Usami, K. Kagawa, K. Kawazoe, Y. Matsumura, H. Sakurai, M. Haruta, Appl. Catal. A 171 (1998) 123.
[7] T. Mishra, K.M. Parida, S.B. Rao, Appl. Catal. A 166 (1) (1998) 115.
[8] S. Imamura, T. Yamashita, R. Hamada, Y. Saito, Y. Nakao, N. Tsuda, C. Kaito, J. Mol. Catal. A 129 (2–3) (1998) 249.
[9] W.H. Cheng, C.Y. Shiau, T.H. Liu, H.L. Tung, J.F. Lu, C.C. Hsu, Appl. Catal. A 170 (1998) 215.
[10] B. Chen, J.L. Farconer, J. Catal. 144 (1993) 214L.
[11] Fun, F.K. Fujimoto, J. Catal. 172 (1997) 238.
[12] Y. Matsumura, K. Tanaka, N. Tode, T. Yazawa, M. Haruta, J. Mol. Catal. A 152 (2000) 157.
[13] Y. Matsumura, N. Tode, Phys. Chem. Chem. Phys. 3 (2001) 1284.
[14] P.B. Rasmussen, M. Kazuta, I. Chorkendorff, Surf. Sci. 318 (1994) 267.
[15] J. Yoshihara, C.T. Campbell, J. Catal. 161 (1996) 776.
[16] J. Yoshihara, S.C. Parker, A. Schfer, C. Campbell, Catal. Lett. 31 (1995) 313.
[17] R. Zhang, A. Ludviksson, C.T. Campbell, Catal. Lett. 25 (1994) 277.

[18] H. Morioka, H. Tagaya, M. Karasu, J. Kadokawa, K. Chiba, Inorg. Chem. 38 (1999) 4211.
[19] N. Tsubaki, M. Ito, K. Fujimoto, J. Catal. 197 (2001) 224.
[20] R. Shiozaki, T. Hayakawa, Y. Liu, T. Ishii, M. Kumagai, S. Hamakawa, K. Suzuki, T. Itoh, T. Shishido, K. Takehira, Catal. Lett. 58 (1999) 131.
[21] G.J. De, A.A. Soler-Illia, R.J. Candal, A.E. Regazzoni, M.A. Blesa, Chem. Mater. 9 (1997) 184.
[22] K. Hashimoto, Y. Hanada, Y. Minami, Y. Kera, Appl. Catal. A 141 (1996) 57.
[23] K. Hashimoto, K. Fukuhara, Y. Fujiwara, H. Kominami, H. Mishima, Y. Kera, Appl. Catal. A 165 (1997) 451.
[24] K. Hashimoto, K. Matsuo, H. Kominami, Y. Kera, J. Chem. Soc., Faraday Trans. 93 (1997) 3729.
[25] K. Hashimoto, N. Toukai, J. Mol. Catal. A 138 (1999) 59.
[26] K. Hashimoto, N. Toukai, J. Mol. Catal. A 161 (2000) 171.
[27] K. Hashimoto, N. Toukai, J. Mol. Catal. A 145 (1999) 273.
[28] G.M. Schwab, A.M. Watson, J. Catal. 4 (1965) 570.
[29] Y. Morokawa, K. Takagi, Y. Morooka, T. Ikawa, Chem. Lett. (1982) 1803.
[30] K. Takahashi, N. Takezawa, H. Kobayashi, Chem. Lett. (1983) 1061.
[31] K. Takahashi, N. Takezawa, H. Kobayashi, Appl. Catal. 2 (1982) 379.
[32] M. Xuhua, L. Guanzhong, Y. Jingfeng, W. Junsong, Cuihua Xuebao 19 (1) (1998) 14.
[33] W.J. Schen, Y. Matsumura, Phys. Chem. Chem. Phys. 2 (2000) 1519.
[34] I.E. Wachs, R.I. Madix, J. Catal. 53 (1978) 208.
[35] C.D. Wagner, et al., Handbook of X-ray Photoelectron Spectroscopy, Perkin Elmer, Eden Prairie, 1979.
[36] A.J. Perrotta, T.J. Garland, Am. Mineral 60 (1975) 152.
[37] P. Scherrer, Göttinger Nachrichten 2 (1918) 98.
[38] R.M. Silberstein, G.C. Bassler, Spectrometric Identification of Organic Compounds, Wiley, 1963, p. 55.
[39] B.A. Sexton, Surf. Sci. 88 (1979) 299.
[40] B.A. Sexton, A.E. Hughes, N.R. Avery, Surf. Sci. 155 (1985) 366.
[41] H. Abe, K. Maruya, K. Domen, T. Onishi, Chem. Lett. (1984) 1875.
[42] G.J. Millar, C.H. Rochester, K.C. Waugh, J. Chem. Soc., Faraday Trans. 87 (1991) 2795.
[43] R. Ryberg, Phys. Rev. B 31 (1985) 2545.
[44] S. Fujita, M. Usui, Catal. Lett. 13 (1992) 349.
[45] S. Fujita, M. Usui, H. Ito, N. Takezawa, J. Catal. 157 (1995) 403.
[46] G.J. Miller, C.H. Rochester, K.C. Waugh, J. Chem. Soc., Faraday Trans. 87 (1991) 1491.
[47] G.J. Miller, J. Catal. 142 (1993) 263.
[48] E. Berello, A. Zecchina, C. Morterra, J. Phys. Chem. 71 (1967) 2938.
[49] R. Burch, S.E. Golunski, M.S. Spencer, J. Chem. Soc., Faraday Trans. 86 (1990) 2683.
[50] R. Burch, S.E. Golunski, M.S. Spencer, Catal. Lett. 5 (1990) 55.
[51] R. Burch, S.E. Golunski, M.S. Spencer, J. Chem. Soc., Faraday Trans. 85 (1) (1989) 3569.
[52] G.J. Millar, C. Rochester, H.S. Bailey, K.C. Waugh, J. Chem. Soc., Faraday Trans. 84 (1992) 2085.
[53] G.J. Millar, C. Rochester, K.C. Waugh, J. Chem. Soc., Faraday Trans. 88 (1992) 2257.
[54] G.J. Millar, C. Rochester, K.C. Waugh, J. Chem. Soc., Faraday Trans. 87 (1992) 1033.
[55] G.J. Millar, C. Rochester, K.C. Waugh, J. Chem. Soc., Faraday Trans. 88 (1992) 3497.
[56] N. Takezawa, H. Kobayashi, A. Hirose, M. Shimokawabe, K. Takahashi, Appl. Catal. 4 (1982) 127.
[57] R. Lefebvre, J. Maruani, J. Chem. Phys. 42 (1965) 1480.
[58] J.H. Lunsford, Catal. Rev. 8 (1973) 135.
[59] R.H. Sand, Phys. Rev. 99 (1955) 1222.
[60] A. Rockenbauer, P. Simon, J. Mag. Reson 11 (1973) 217.
[61] J.Y. Yan, G.-D. Lei, W.M.H. Sachtler, H.H. Kung, J. Catal. 161 (1996) 43.
[62] P.J. Carl, S.C. Larsen, J. Catal. 182 (1999) 208.
[63] R.J. Feber, M.T. Rogers, J. Am. Chem. Soc. 81 (1959) 1849.
[64] A. Nicula, D. Stamires, J. Turkevich, J. Chem. Phys. 42 (1965) 3684.